CRYSTAL
GROWTH
& DESIGN

Ligand-Structure Effect on the Formation of One-Dimensional Nanoscale Cu(II)-Schiff Base Complexes and Solvent-Mediated Shape Transformation

Wenjing Wang,[†] Qianhuo Chen,*[,†,‡] Qing Li,[†] Yu Sheng,[†] Xuanjun Zhang,*[,§] and Kajsa Uvdal*[,§]

[†]College of Environmental Science and Engineering, Fujian Normal University, Fuzhou 350007, P. R. China

[‡]Fujian Key Laboratory of Polymer Materials, Fuzhou 350007, P. R. China

[§]Division of Molecular Surface Physics and Nanoscience, Department of Physics, Chemistry, and Biology (IFM), Linköping University, Linköping 58183 Sweden

Supporting Information

ABSTRACT: We report here a Cu(II)-Schiff base complex that can assemble into one-dimensional (1D) nanoscale fibers, belts, and rods under different synthetic conditions. The ligand-structure effect is investigated by modification of the ligand structure. The formation of a 1D nanostructure was studied, and the formation of dimers was revealed as a key factor for 1D assembly. In dimethylformamide (DMF) medium, this complex represents one of the rare examples of low-molecular-weight "super-metallogelators" with a critical gelation concentration of 0.3 wt % for DMF. The ligand exhibits good selectivity toward different metal ions in terms of gel formation and only the Cu(II) complex forms gels. It is interesting that this metallogel is a kind of dynamic nanostructure, which can be transformed to rods with different aspect ratios via a solvent-mediated process under stimulation of ultrasound.

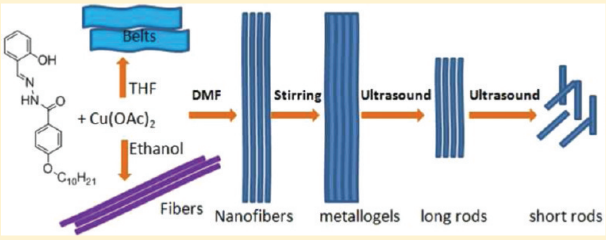

■ INTRODUCTION

Supramolecular organization of randomly oriented molecules into long-range ordered nanostructured materials is an important goal for developing nanodevices, sensors, molecular circuitry, and machines.[1] In particular, coordination-directed assembly has evolved as an attractive strategy for fabricating functional materials because the coordination number, geometry, and oxidation state of the metal centers play significant roles in controlling the size, shape, and physical and chemical properties of the final nanomaterials.[2] Several recent studies showed that nanoparticles of metallopolymers and metal−organic frameworks (MOFs) exhibit promising functionalities such as ion exchange,[3] accelerated guest adsorption,[4] magnetism,[5] multimodal bioimaging,[6] drug delivery and sensing,[7] field emission,[8] encapsulation of functional guest molecules,[9,10] and enhanced fluorescence and/or light harvesting.[10] The properties of these nanomaterials always depend on the particle sizes and shapes, as well as molecular arrangements.

Nanoscale one-dimensional (1D) coordination complexes and polymers such as fibers, belts, rods, and tubes are an exciting class of materials with excellent potential for nanosized electronic, mechanical, and medical fields. However, despite the advances that have been achieved, methods for controlling particle size and shape of coordination complex/polymers are still fairly rudimentary.[2] 1D nanostructured coordination complexes and polymers are still very scarce.[2,11] Metallogels, a kind of new emerging smart metal-containing nanomaterial always formed by interfiber interaction that can trap immobilize solvent molecules, has gained attention until very recently.[2e,12−15] Therefore, development of new synthesis methods of 1D nanoscale coordination assemblies and understanding the formation mechanism at the molecular level are significantly important for the rational design of functional materials for electronic, optical, and biological applications. We present herein a molecular approach to metal-containing gels, belts, fibers, and rods of a Cu(II)-Schiff base coordination complex (Scheme 1). The metallogel is a dynamic nanostructure, which exhibits solvent-mediated shape transformation to nanorods under stimulation of ultrasound.

■ EXPERIMENTAL SECTION

Materials and Methods. All of the chemicals were purchased from Sinopharm Chemical Reagent Co., Ltd. and used without further purification. UV−visible spectra were recorded on a Varian CARY 50 spectrometer. IR spectra were collected on a Nicolet 5700 spectrometer (using KBr pellets). NMR analysis was performed on Bruker AVIII-400 instruments. Elemental analysis (C, H, N) was performed using varioEL III analyzer. Scanning electron microscopy (SEM) and transmission electron microscopy (TEM) images were obtained using a JEOL JSM-7500F (field emission scanning electron microscope) and FEI Tecnai G2 microscope, respectively. X-ray diffraction (XRD) patterns were recorded on a Panalytical X'Pert

Received: March 20, 2012
Revised: March 28, 2012
Published: April 2, 2012

dx.doi.org/10.1021/cg300372v | *Cryst. Growth Des.* 2012, 12, 2707−2713

Scheme 1. Molecular Structures of Ligands and Illustration of Shape Control and Transformation of One-Dimensional Nanostructures

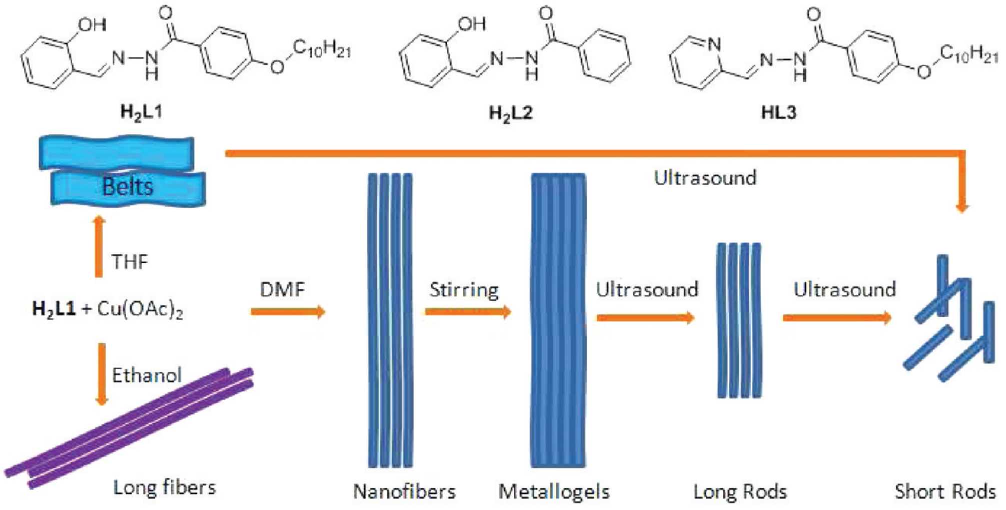

spectrometer using Co Kα radiation (λ = 1.78897 Å) and the data were converted to Cu Kα data. Ultrasonic reaction was performed with KQ-250B (40 kHz) ultrasonic cleaning sonicator. Electrospray ionization (ESI) mass spectra were recorded on BRUKER ESQUIRE 3000 PLUS spectrometer using methanol as the solvent.

Synthesis of 1. A flask was charged with a mixture of methyl 4-hydroxybenzoate (12.78 g, 84 mmol), 1-bromodecane (16.6 mL, 80 mmol), and K_2CO_3 (30 g, excess). Dimethylformamide (DMF) (120 mL) was added. The flask was degassed by bubbling with nitrogen for 10 min. The mixture was heated at 90 °C with magnetic stirring for two days. After cooling to room temperature, water (250 mL) and ethyl acetate (250 mL) were added and stirred for 5 min. The organic layer was separated, washed with 10% Na_2CO_3 and water two times, and dried over anhydrous $MgSO_4$. Then the solid was removed by filtration, and the filtrate was evaporated to remove ethyl acetate. After cooling to room temperature, a pale yellow product was obtained. Yield: 20.86 g, 89% (based on 1-bromodecane). ^{1}HNMR (400 MHz, $CDCl_3$): δ = 7.98 (d, J = 8.9 Hz, 2H, Ar–H), 6.90 (d, J = 8.9 Hz, 2H, Ar–H), 4.00 (t, J = 6.6 Hz, 2H, -OCH_2), 3.88 (s, 3H, -OCH_3), 1.77–1.82 (m, 2H, –CH_2), 1.24–1.46 (m, 14H, -C_7H_{14}), 0.88 (t, J = 6.5 Hz, 3H, –CH_3).

Synthesis of 2. A flask was charged with a mixture of **1** (20.00 g, 68.5 mmol) and hydrazine hydrate (40 mL, excess). EtOH (100 mL) was added. The flask was degassed by bubbling with nitrogen for 10 min. The mixture was refluxed at 80 °C with magnetic stirring for two days. After cooling to room temperature, water (500 mL) was added. The precipitate was collected by filtration, washed with water four times and with ethanol/water = 1:4 three times. Then a white product was dried in a vacuum desiccator. Yield: 17.7 g, 89% (based on 1). ^{1}HNMR (400 MHz, DMSO): δ = 9.61 (s, 1H, -NH), 7.71–7.84 (m, 2H, Ar–H), 6.90–7.03 (m, 2H, Ar–H), 4.53 (broad, 2H, NH_2), 4.01 (m, 2H, -OCH_2), 1.53–1.86 (m, 2H, –CH_2), 1.12–1.49 (m, 14H, -C_7H_{14}), 0.85 (t, J = 6.9 Hz, 3H, –CH_3).

Synthesis of H_2L1. A flask was charged with a mixture of **2** (2.00 g, 6.8 mmol) and 2-hydroxybenzaldehyde (0.7 mL, 6.8 mmol). EtOH (40 mL) was added. The flask was degassed by bubbling with nitrogen for 10 min. The mixture was refluxed at 80 °C with magnetic stirring for 8 h. After cooling to room temperature, a white precipitate was obtained. The precipitate was collected by filtration and washed with ethanol/water = 1:1 three times. The white product was dried in a vacuum desiccator. Yield: 2.45 g, 91%. ^{1}HNMR(400 MHz, DMSO): δ = 11.98 (s, 1H, -NH), 11.38 (s, 1H, –OH), 8.62 (s, 1H, -NCH), 7.92 (d, J = 8.5 Hz, 2H, Ar–H), 7.52 (d, J = 7.5 Hz, 1H, Ar–H), 7.30 (t, J = 7.7 Hz, 1H, Ar–H), 7.12–6.81 (m, 4H, Ar–H), 4.05 (t, J = 6.5 Hz, 2H, -OCH_2), 1.79–1.60 (m, 2H, –CH_2), 1.48–1.12 (m, 14H, -C_7H_{14}), 0.86 (t, J = 6.8 Hz, 3H, –CH_3). ^{13}CNMR (100 MHz, DMSO): δ = 162.64, 162.15, 158.00, 148.34, 131.59, 130.08, 125.02, 119.69, 119.14, 116.86, 114.62, 68.22, 31.80, 29.71–28.97, 25.96, 22.58, 14.37. Anal. Calcd (%) for $C_{24}H_{32}N_2O_3$: C, 72.7; H, 8.1; N, 7.1. Found (%): C,72.7, H, 8.0, N, 6.9. MS (m/z) calc. for $C_{24}H_{32}N_2O_3$: 396.2; Found: 397.0 [M + H]$^+$.

Scheme 2. Synthesis Route of H_2L1

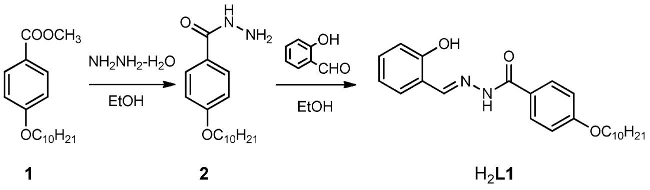

Synthesis of H_2L2. A flask was charged with a mixture of benzhydrazide (2.00 g, 14.7 mmol) and 2-hydroxybenzaldehyde (1.6 mL, 15 mmol). EtOH (30 mL) was added. The flask was degassed by bubbling with nitrogen for 10 min. The mixture was refluxed at 80 °C with magnetic stirring for 8 h. After cooling to room temperature, a yellow precipitate was obtained. The precipitate was collected by filtration and washed with ethanol three times. The deep yellow crystals were dried in a vacuum desiccator. Yield: 2.8 g, 80%. ^{1}H NMR (400 MHz, DMSO): δ = 12.11 (s, 1H, -NH), 11.30 (s, 1H, –OH), 8.66 (s, 1H, -NCH), 7.95 (d, J = 7.3 Hz, 2H, Ar–H), 7.54–7.64 (m, 4H, Ar–H), 7.32 (t, J = 7.3 Hz, 1H, Ar–H), 6.94 (t, J = 8.8 Hz, 2H, Ar–H). Anal. Calcd (%) for $C_{14}H_{12}N_2O_2$: C, 69.99; H, 5.03; N, 11.66. Found (%): C, 70.15; H, 4.93; N, 11.02. MS (m/z) calc. for $C_{14}H_{12}N_2O_2$: 240.1; Found: 263.76 [M + Na]$^+$.

Synthesis of HL3. A flask was charged with a mixture of **2** (2.00 g, 6.8 mmol) and picolinaldehyde (0.7 mL, 6.8 mmol). EtOH (40 mL) was added. The flask was degassed by bubbling with nitrogen for 10 min. The mixture was refluxed at 80 °C with magnetic stirring for 8 h. After cooling to room temperature, a white precipitate was obtained. The precipitate was collected by filtration and washed with ethanol three times. The white product was dried in a vacuum desiccator. Yield: 2.36 g, 91%. ^{1}H NMR (400 MHz, DMSO): δ = 11.92 (s, 1H, -NH), 8.62 (d, J = 4.8 Hz, 1H, pyridine-H), 8.47 (s, 1H, -NCH), 7.84 – 8.03 (m, 4H, pyridine-H, Ar–H), 7.36–7.46 (m, 1H, pyridine-H), 7.06 (d, J = 8.8 Hz, 2H, Ar–H), 4.05 (t, J = 6.5 Hz, 2H, -OCH_2), 1.55 – 1.75 (m, 2H, –CH_2), 1.15 – 1.52 (m, 14H, -C_7H_{14}), 0.86 (t, J = 6.7 Hz, 3H, –CH_3). ^{13}CNMR(100 MHz, $CDCl_3$): δ = 162.29, 153.25, 148.99, 136.56, 129.78, 124.65, 124.08, 114.17, 68.17, 31.89, 30.93, 29.34, 25.99, 22.67, 14.11. Anal. Calcd (%) for $C_{23}H_{31}N_3O_2$: C, 72.4;

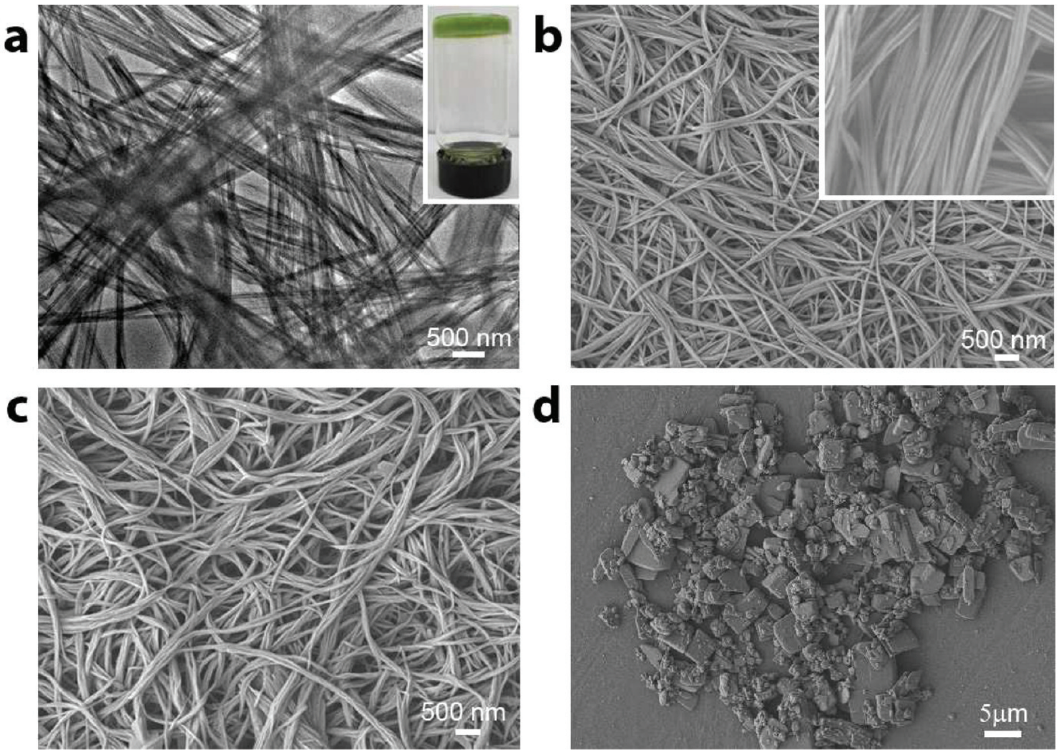

Figure 1. (a) TEM image of Cu-**L1** gels formed in DMF; inset: photoimage of the gels; (b) SEM image of Cu-**L1** gels formed in DMF; inset: enlarged view of nanofiber bundles; (c) SEM image of Cu-**L1** nanofibers synthesized from dilute DMF solution by addition of water; (d) SEM image of Cu-**L3** particles.

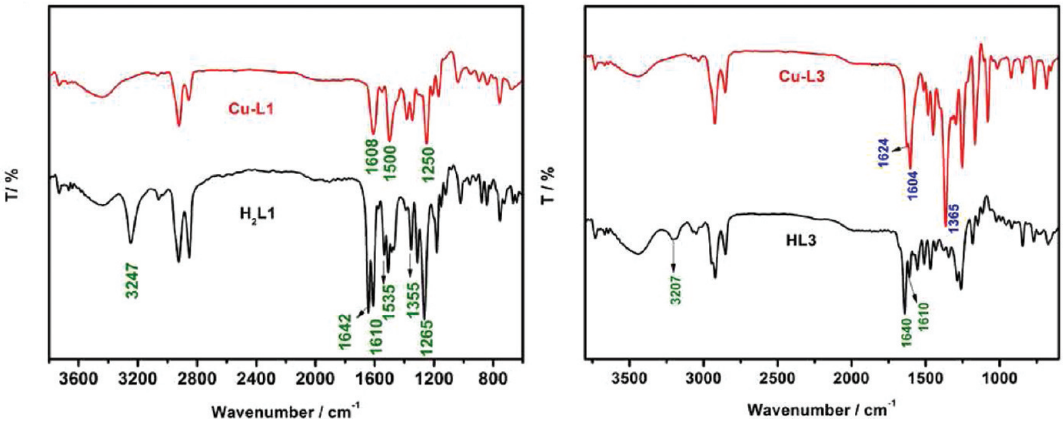

Figure 2. IR data of H_2**L1**, Cu-**L1**, H**L3**, and Cu-**L3**.

H, 8.2; N, 11.0. Found (%): C, 72.2; H, 8.1; N, 10.4. MS (*m/z*) cacl. for $C_{23}H_{31}N_3O_2$: 382.2; Found: 382.0 $[M + H]^+$.

Synthesis of Cu-L1. A DMF solution of $Cu(OAc)_2{\cdot}H_2O$ (0.02 mmol, 0.5 mL) was added into a solution of H_2**L1** (0.01 M, 1 mL) in DMF under stirring at room temperature for 30 min and green gels were obtained. The nanofibers were washed with ethanol three times and redispersed in ethanol for SEM and TEM analysis. For elemental analysis (C, H, N), the powder was dried in a vacuum desiccator for three days before measurement. Yield: 67%. Anal. Calcd (%) for $C_{24}H_{30}CuN_2O_3$: C, 62.95; H, 6.56; N, 6.12. Found (%): C, 62.91; H, 6.49; N, 5.61. Long and short nanorods of Cu-**L1** were obtained by ultrasonication of as-prepared Cu-**L1** gel in DMF for 15 and 60 min, respectively. The nanorods were collected by centrifugation and washed with ethanol and dried in a vacuum.

Synthesis of Cu-L2. H_2**L2** (0.02 mmol, 4.8 mg) was dissolved in ethanol (5 mL) and a solution of $Cu(OAc)_2{\cdot}H_2O$ (0.02 mmol, 4.0 mg) in ethanol (5 mL) was added dropwise under stirring. The mixture was further stirred for 30 min and the resulting green precipitate was collected by centrifugation and washed with ethanol three times. Yield: 87%. Anal. Calcd (%) for ($C_{14}H_{10}CuN_2O_2$): C, 55.72; H, 3.34; N, 9.28. Found(%): C, 55.80; H, 3.31; N, 8.76.

Synthesis of Cu-L3. H**L3** (0.01 mmol, 3.8 mg) was dissolved in DMF (1 mL), $Cu(OAc)_2{\cdot}H_2O$ (0.01 mmol, 2 mg) in DMF (0.5 mL) was added. The mixture was stirred for 30 min at room temperature and the powder was collected by centrifugation and washed with ethanol three times. Yield: 51%. Anal. Calcd (%) for $C_{25}H_{33}CuN_3O_4$: C, 59.70; H, 6.57; N, 8.36. Found (%): C, 59.75; H, 6.50; N, 7.73.

RESULTS AND DISCUSSION

As shown in Scheme 1, H_2**L1** is a three dentate chelating ligand. The addition of long alkyl chains is expected to promote cross-linking between molecular stacks and thus effectively modulate the final morphologies.[2e,10g] Addition of an DMF solution of $Cu(OAc)_2$ (0.02 M, 0.5 mL) into a solution of H_2**L1** in DMF (0.01 M, 1 mL) resulted in green precipitate in 10 min, which

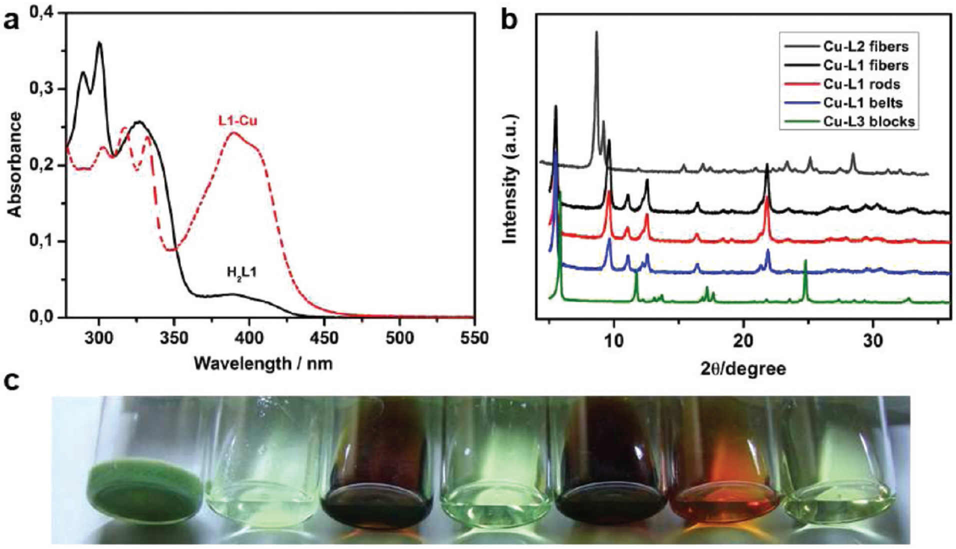

Figure 3. (a) UV−vis absorption of H_2**L1** and Cu-**L1**. (b) XRD data of Cu-**L1** fibers, rods, and belts, Cu-**L2** nanofibers, and Cu-**L3** particles. (c) Photoimage of H_2**L1** after the addition of different metal ions, from left to right: Cu^{2+}, Zn^{2+}, Co^{2+}, Cd^{2+}, Mn^{2+}, Ni^{2+}, Li^{+}.

forms gels after further stirring for 30 min at room temperature. The gel formation can be promoted by increasing the precursor concentrations. For example, gels can be obtained within 4 min when the concentrations of $Cu(OAc)_2$ and H_2**L1** are increased to 0.04 and 0.02 M, respectively. TEM and SEM analyses reveal that the gels consist of aligned nanofibers with widths of 80 nm and lengths up to hundreds of micrometers (Figures 1a,b and S1, Supporting Information). In fact, Cu-**L1** acts as a "supergelators"[12,13] with critical gelation concentration of 0.3 wt % for DMF, which represents one of the rare examples of metallogelators with low molecular weight.

When the precursor solution is dilute, no precipitate is observed. For example, mixing of H_2**L1** (2×10^{-3} M, 1 mL) and $Cu(OAc)_2$ (4×10^{-3} M, 0.5 mL) leads to a clear solution. Interestingly, nanofibers can also be obtained after addition of water into this precursor solution (Figure 1c). Commonly, spherical amorphous particles precipitate after addition of nonsolvents such as water or ether into a precursor solution containing ligands and metal ions.[2] The formation of nanofibers after addition of water in this system indicates that the unidirectional intermolecular forces are strong enough to overcome the rapid and random aggregation of coordination complexes and effectively modulate the final morphology.

Infrared spectrum (Figure 2) of Cu-**L1** dried powder does not play the amide C═O (1642 cm^{-1}) stretch and peak for NH at 3247 cm^{-1}. The intensity increase at 390 nm in the UV−vis absorption spectrum of Cu-**L1** indicates the extension of π−conjugation in the whole ligand (Figure 3a). These results indicate that H_2**L1** is deprotonated to coordinate with Cu(II) in the enolate form. Elemental analysis revealed the ratio between ligand and Cu(II) is 1:1. XRD analysis revealed that the nanofibers exhibit sharp diffraction peaks, indicative of high crystallinity (Figure 3b). The ligand exhibits good selectivity toward different metal ions in term of metallogel formation. As shown in Figure 3c, after the addition of different metal acetate salts (Cu^{2+}, Zn^{2+}, Co^{2+}, Cd^{2+}, Mn^{2+}, Ni^{2+}, Li^{+}), only Cu-**L1** gel was observed.

As revealed from our experiment results, the formation of gels is about 30 min later than nanofibers, which indicates that the growth along the 1D direction is fast and predominant in the first stage. To study the mechanism of 1D assembly, we further synthesized ligands H_2**L2** and H**L3**. H_2**L2** has the same chelating moiety with that of H_2**L1** but it has no alkyl chain. Addition of an ethanol solution of $Cu(OAc)_2$ into a solution of H_2**L2** in ethanol resulted in green precipitate. SEM analysis revealed that the Cu-**L2** particles are also nanofibers with diameters of 90 nm and lengths up to hundreds of micrometers (Supporting Information, Figure S2). No precipitation was observed when DMF was used as the solvent due to the good solubility in this solvent. Interestingly, nanofibers were also obtained by the addition of water into a DMF solution of the precursors. This result reveals that the chelating moiety plays a key role in the coordination-induced assembly of the 1D nanostructure.

To investigate this mechanism at the molecular level, electrospray ionization (ESI) mass spectrometry was performed. Figure 4 shows the ESI data of Cu-**L2** measured using methanol as the solvent. The main peak at 602.9 (m/z) can be assigned to $Cu_2(\mathbf{L2})_2$, which indicates that there are dimers formed even in the dilute solution. Similarly, the dimer formation was also observed from the ESI data of the Cu-**L1** complex. On the basis of the experimental results, the formation of the 1D nanostructure was proposed. As shown in Scheme 1 and Figure 5, H_2**L1** is a tridentate chelating ligand, which can form a neutral complex with Cu(II) ions in a molar ratio of 1:1. However, this ligand could not saturate the coordination numbers if they formed a neutral mononuclear complex. As a result, the complexes may form dimers, which then assemble into supramolecular structures by sharing some coordinating atoms (or linked by sharing coordinating atoms of solvent molecules) to saturate the coordination of Cu(II).

To further investigate this formation mechanism, comparison ligand H**L3** was synthesized. H**L3** is also a tridentate ligand. The difference is that **L3** is a negatively charged monovalent ligand when coordinated with Cu(II). Under the same preparation condition with that of Cu-**L1**, microscale block crystals of Cu-**L3** were obtained (Figure 1d). Elemental analysis and IR data revealed that Cu-**L3** has a formula of $Cu(CH_3COO)$**L3**. Because **L3** is a monovalent tridentate chelating ligand, an acetate anion further binds to Cu(II) (via

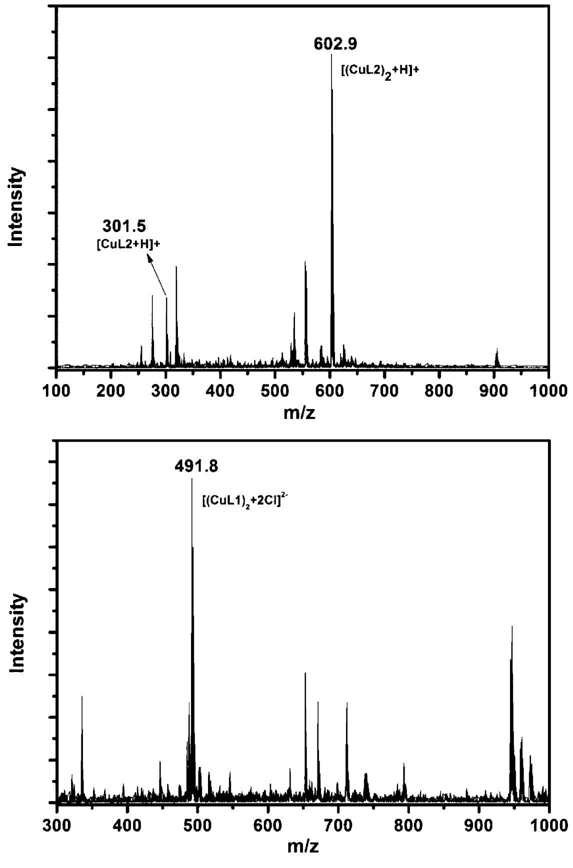

Figure 4. ESI-MS data of Cu-**L1** and Cu-**L2** showing the dimer formation in dilute solution.

monodentate coordination mode, $\nu_{as} - \nu_{s} = 239$ cm^{-1}, Figure 2) to saturate the coordination number of Cu(II) and also balance the charge of the complex. Therefore, there is less possibility for the Cu atom to further share coordinating atoms with neighboring molecules to form polymeric structures. Another comparison experiment (Cu-**L1**) was performed in DMF in the presence of pyridine. Because excess pyridine can easily saturate the coordination number of Cu atom in the Cu-**L1** monomer, it is unnecessary for Cu atom to form dimers and further share coordinating atoms with neighboring molecules, and therefore no 1D nanostructure is expected. In our experiment, three drops of pyridine was premixed with H_2**L1** (0.02 M, 1 mL) before addition of $Cu(OAc)_2$ (0.04 M, 0.5 mL). Experimental results showed that neither precipitate nor gels were formed, which again supports the proposed mechanism.

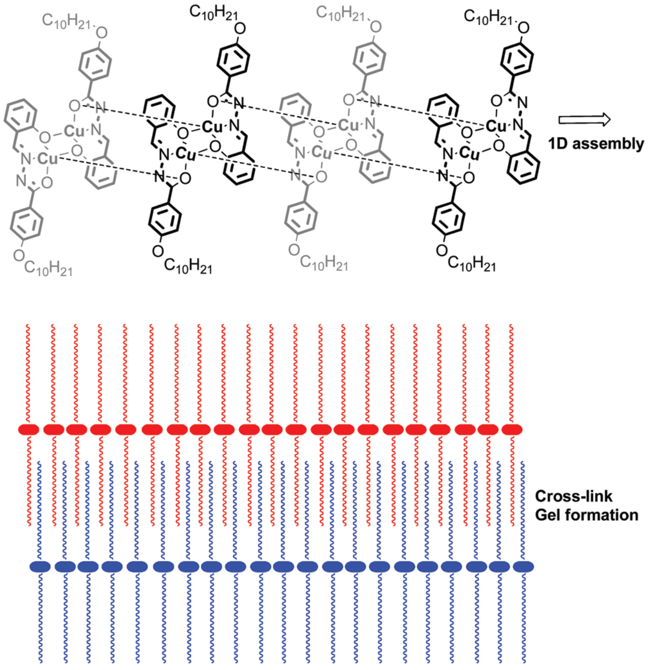

Figure 5. Proposed 1D supramolecular structure and schematic illustration of gel formation.

Ultrasound and solvents can effectively tune the particle sizes and aspect ratio of the 1D nanostructure. When the experiment was performed in THF, belt-shaped crystals were obtained. As shown in Figure 6a, the particles exhibit an average width 0.5 μm, thickness of 80 nm, and lengths up to hundreds of micrometers. Compared with those in DMF and THF, the formation of nanofibers in an ethyl acetate system is much faster and the width of fibers is much thinner (ca. 40 nm). This probably results from the low solubility of Cu-**L1** in ethyl acetate, which induces the unidirectional growth rapidly (Figure 6b).

Cu-**L1** gels here are a dynamic nanostructure, which exhibit shape transformation under stimulation of ultrasound. For example, 15 min of ultrasonication of the gels in DMF leads to long nanorods with a width of 80 nm and average lengths of 4 μm as revealed by SEM measurement (Figure 6c). Longer time of ultrasonication leads to further shorter rods. Figure 6d shows the SEM image of nanorods obtained after 1 h of ultrasonication, which have an average width of ~85 nm and lengths of 1−1.5 μm. XRD analysis revealed that both of the nanowires and nanorods exhibit sharp and very similar diffraction peaks, indicative of high crystallinity (Figure 3b). It is interesting that the nanobelts synthesized in THF also exhibit this shape transformation upon stimulation of ultrasound. The aspect ratio of nanofibers prepared from ethyl acetate and that precipitated from DMF dilute solution by the addition of water do not show any change after ultrasonication. When these nanofibers (collected by centrifugation) were dispersed in DMF or THF, they exhibited shape transformation under stimulation of ultrasound. The effect of DMF and THF is probably owing to the relatively better solubility of Cu-**L1** in DMF and THF than those in ethyl acetate and water, which may facilitate this solvent-mediated shape transformation.

In conclusion, we have demonstrated a supramolecular approach to nanoscale metal-containing gels, fibers, belts, and rods. The ligand-structure effect and mechanism of 1D growth of nanofibers have been studied. In this system, dimer formation was found to be a key factor for the 1D supramolecular assemblies. Cu-**L1** acts as "super-gelators" representing one of the rare examples of metallogelators with low molecular weight. The dynamic metal-containing gels and nanofibers formed by supramolecular assembly exhibit solvent-mediated shape transformation by stimulation of ultrasound. The shape control and the study of the structure effect at the molecular level in this work will certainly expand the synthesis of 1D metal-containing nanostructure in the development of new functional materials.

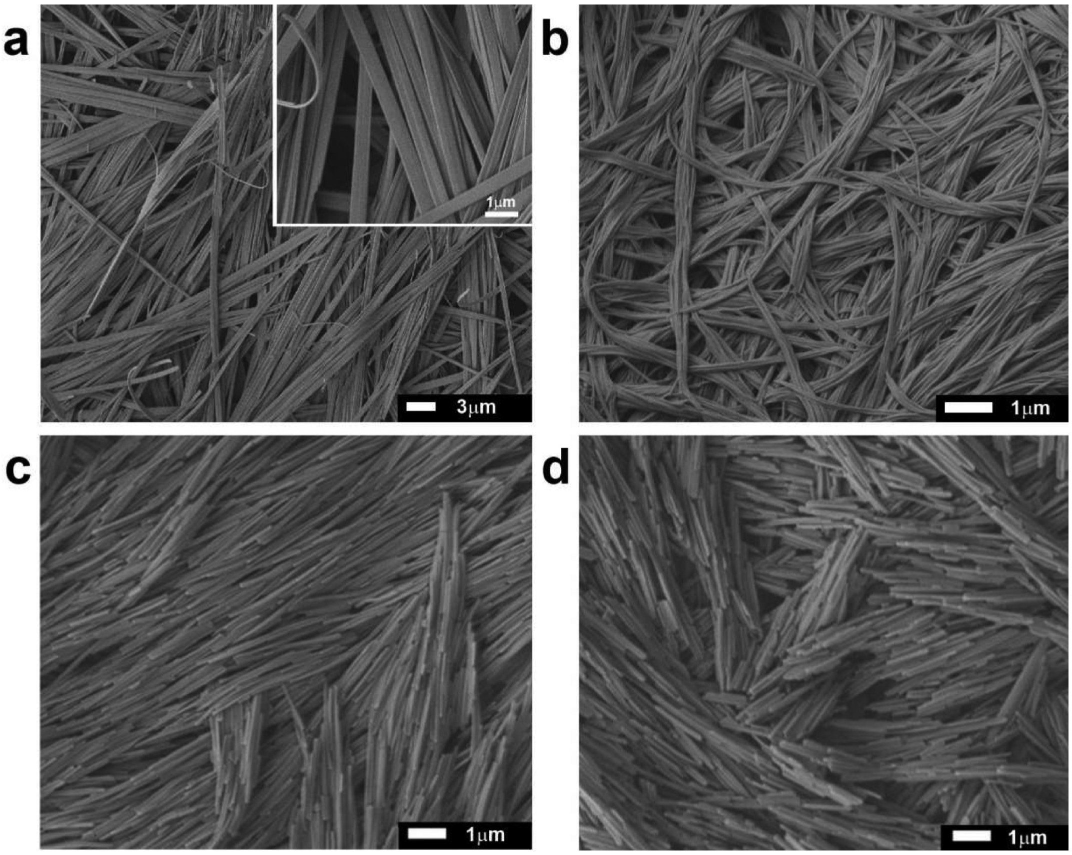

Figure 6. SEM images of Cu-**L1** prepared under different conditions: (a) in THF with ultrasonication for 7 min; (b) in ethyl acetate with stirring for 15 min; (c) in DMF under ultrasonication for 15 min; (d) in DMF under ultrasonication for 1 h.

■ ASSOCIATED CONTENT

Ⓢ Supporting Information

SEM images. This material is available free of charge via the Internet at http://pubs.acs.org.

■ AUTHOR INFORMATION

Corresponding Author

*E-mail: qhchen@fjnu.edu.cn (Q.C.); xuazh@ifm.liu.se (X.Z.); kajsa@ifm.liu.se (K.U.).

Notes

The authors declare no competing financial interest.

■ ACKNOWLEDGMENTS

The authors are indebted to the financial support of Natural Scientific Foundation of Fujian Province of China (No. A0710001); the Education Department of the Fujian Province of China (No. JB10010); the Swedish Foundation for Strategic Research (SSF) within the Nano-X program (Grant No. SSF [A3 05:204]), and Swedish government strategic faculty grant in material science (SFO, MATLIU) in Advanced Functional Materials (AFM).

■ REFERENCES

(1) (a) Fegan, A.; White, B.; Carlson, J. C. T.; Wagner, C. R. *Chem. Rev.* **2010**, *110*, 3315−3336. (b) Whitesides, G. M.; Grzybowski, B. *Science* **2002**, *295*, 2418−2421. (c) Mann, S. *Nat. Mater.* **2009**, *8*, 781−792. (d) Kim, H.-J.; Kim, T.; Lee, M. *Acc. Chem. Res.* **2011**, *44*, 72−82. (e) Carnall, J. M. A.; Waudby, C. A.; Belenguer, A. M.; Stuart, M. C. A.; Peyralans, J. J.-P.; Otto, S. *Science* **2010**, *327*, 1502−1506.

(2) See recent reviews: (a) Leong, W. L.; Vittal, J. J. *Chem. Rev.* **2011**, *111*, 688−764. (b) Lin, W.; Rieter, W. J.; Taylor, K. M. L. *Angew.Chem., Int. Ed.* **2009**, *48*, 650−658. (c) Spokoyny, A. M.; Kim, D.; Sumrein, A.; Mirkin, C. A. *Chem. Soc. Rev.* **2009**, *38*, 1218−1227. (d) Wang, X.; McHale, R. *Macromol. Rapid Commun.* **2010**, *31*, 331−350. (e) Hui, J. K.-H.; MacLachlan, M. J. *Coord. Chem. Rev.* **2010**, *254*, 2363−2390. (f) Carné, A.; Carbonell, C.; Imaz, I.; Maspoch, D. *Chem. Soc. Rev.* **2011**, *40*, 291−305. (g) Whittell, G. R.; Hager, M. D.; Schubert, U. S.; Manners, I. *Nat. Mater.* **2011**, *10*, 176−188.

(3) (a) Oh, M.; Mirkin, C. A. *Nature* **2005**, *438*, 651−654. (b) Oh, M.; Mirkin, C. A. *Angew. Chem., Int. Ed.* **2006**, *45*, 5492−5494.

(4) Tanaka, D.; Henke, A.; Albrecht, K.; Moeller, M.; Nakagawa, K.; Kitagawa, S.; Groll, J. *Nat. Chem.* **2010**, *2*, 410−416.

(5) Catala, L.; Brinzei, D.; Prado, Y.; Gloter, A.; Stéphan, O.; Rogez, G.; Mallah, T. *Angew. Chem., Int. Ed.* **2009**, *48*, 183−187.

(6) (a) Liu, D.; Huxford, R. C.; Lin, W. *Angew. Chem., Int. Ed.* **2011**, *50*, 3696−3700. (b) deKrafft, K. E.; Xie, Z.; Cao, G.; Tran, S.; Ma, L.; Zhou, O. Z.; Lin, W. *Angew. Chem., Int. Ed.* **2009**, *48*, 9901−9904. (c) Taylor, K. M. L.; Rieter, W. J.; Lin, W. *J. Am. Chem. Soc.* **2008**, *130*, 14358−14359. (d) Taylor, K. M. L.; Jin, A.; Lin, W. *Angew. Chem., Int. Ed.* **2008**, *47*, 7722−7725. (e) Rieter, W. J.; Taylor, K. M. L.; An, H.; Lin, W.; Lin, W. *J. Am. Chem. Soc.* **2006**, *128*, 9024−9025.

(7) (a) Rieter, W. J.; Pott, K. M.; Taylor, K. M. L.; Lin, W. *J. Am. Chem. Soc.* **2008**, *130*, 11584−11585. (b) Rieter, W. J.; Taylor, K. M. L.; Lin, W. *J. Am. Chem. Soc.* **2007**, *129*, 9852−9853. (c) Taylor-Pashow, K. M. L.; Rocca, J. D.; Xie, Z.; Tran, S.; Lin, W. *J. Am. Chem. Soc.* **2009**, *131*, 14261−14263.

(8) Batabyal, S. K.; Peedikakkal, A. M. P.; Ramakrishna, S.; Sow, C. H.; Vittal, J. J. *Macromol. Rapid Commun.* **2009**, *30*, 1356−1361.

(9) (a) Imaz, I.; Hernando, J.; Ruiz-Molina, D.; Maspoch, D. *Angew. Chem., Int. Ed.* **2009**, *48*, 2325−2329. (b) Champness, N. R. *Angew. Chem., Int. Ed.* **2009**, *48*, 2274−2275. (c) Yan, Y.; Martens, A. A.;

Besseling, N. A. M.; de Wolf, F. A.; de Keizer, A.; Drechsler, M.; Stuart, M. A. C. *Angew. Chem., Int. Ed.* **2008**, *47*, 4192−4195.

(10) (a) Nishiyabu, R.; Aimé, C.; Gondo, R.; Noguchi, T.; Kimizuka, N. *Angew. Chem., Int. Ed.* **2009**, *48*, 9465−9468. (b) Aime, C.; Nishiyabu, R.; Gondo, R.; Kaneko, K.; Kimizuka, N. *Chem. Commun.* **2008**, 6534−6536. (c) Aimé, C.; Nishiyabu, R.; Gondo, R.; Kimizuka, N. *Chem.—Eur. J.* **2010**, *16*, 3604−3607. (d) Nishiyabu, R.; Aimé, C.; Gondo, R.; Kaneko, K.; Kimizuka, N. *Chem. Commun.* **2010**, *46*, 4333−4335. (e) Zhang, X.; Ballem, M. A.; Ahrén, M.; Suska, A.; Bergman, P.; Uvdal, K. *J. Am. Chem. Soc.* **2010**, *132*, 10391−10397. (f) Zhang, X.; Chen, Z.-K.; Loh, K. P. *J. Am. Chem. Soc.* **2009**, *131*, 7210−7211. (g) Zhang, X.; Ballem, M. A.; Zhang, J.-H.; Bergman, P.; Uvdal, K. *Angew. Chem., Int. Ed.* **2011**, *50*, 5847−5851. (h) Liu, K.; You, H.; Jia, G.; Zheng, Y.; Huang, Y.; Song, Y.; Yang, M.; Zhang, L.; Zhang, H. *Cryst. Growth Des.* **2010**, *10*, 790−797.

(11) (a) Imaz, I.; Rubio-Martínez, M.; Saletra, W. J.; Amabilino, D. B.; Maspoch, D. *J. Am. Chem. Soc.* **2009**, *131*, 18222−18223. (b) Chen, Y.; Li, K.; Lloyd, H. O.; Lu, W.; Chui, S. S.-Y.; Che, C.-M. *Angew. Chem., Int. Ed.* **2010**, *49*, 9968−9971. (c) Kuhn, P.; Puigmartí-Luis, J.; Imaz, I.; Maspoch, D.; Dittrich, P. S. *Lab Chip* **2011**, *11*, 753−757. (d) Puigmartí-Luis, J.; Rubio-Martínez, M.; Hartfelder, U.; Imaz, I.; Maspoch, D.; Dittrich, P. S. *J. Am. Chem. Soc.* **2011**, *133*, 4216−4219. (e) Kaminker, R.; Popovitz-Biro, R.; van der Boom, M. E. *Angew. Chem., Int. Ed.* **2011**, *50*, 3224−3226.

(12) (a) Terech, P.; Weiss, R. G. *Chem. Rev.* **1997**, *97*, 3133−3159. (b) Estroff, L. A.; Hamilton, A. D. *Chem. Rev.* **2004**, *104*, 1201−1217. (c) Sangeetha, N. M.; Maitra, U. *Chem. Soc. Rev.* **2005**, *34*, 821−836. (d) Special issue: Low Molecular Mass Gelators. Design, Self-Assembly, Function; Fages, F., Ed. *Top. Curr. Chem.* **2005**, 256. (e) *Molecular Gels: Materials with Self-Assembled Fibrillar Networks*; Weiss, R. G.; Terech, P, Eds.; Kluwer Academic Publishers: Dordrecht, 2005. (f) Llusar, M.; Sanchez, C. *Chem. Mater.* **2008**, *20*, 782−820.

(13) (a) Fages, F. *Angew. Chem., Int. Ed.* **2006**, *45*, 1680−1682. (b) Adarsh, N. N.; Sahoo, P.; Dastidar, P. *Cryst Growth Des.* **2010**, *10*, 4976−4986.

(14) (a) Hui, J. K.-H.; Yu, Z.; MacLachlan, M. J. *Angew. Chem., Int. Ed.* **2007**, *46*, 7980−7983. (b) Leong, W. L.; Tam, A. Y. Y.; Batabyal, S. K.; Koh, L. W.; Kasapis, S.; Yam, V. W. W.; Vittal, J. J. *Chem. Commun.* **2008**, 2628−3630. (c) Komiya, N.; Muraoka, T.; Iida, M.; Miyanaga, M.; Takahashi, K.; Naota, T. *J. Am. Chem. Soc.* **2011**, *133*, 16054−16061. (d) Liu, J.; He, P.; Yan, J.; Fang, X.; Peng, J.; Liu, K.; Fang, Y. *Adv. Mater.* **2008**, *20*, 2508−2511. (e) Liu, T.; Hu, J.; Yin, J.; Zhang, Y.; Li, C.; Liu, S. *Chem. Mater.* **2009**, *21*, 3439−3446. (f) Tu, T.; Fang, W.; Bao, X.; Li, X.; Dötz, K. H. *Angew. Chem., Int. Ed.* **2011**, *50*, 6601−6605. (g) Strassert, C. A.; Chien, C.-H.; Lopez, M. D. G.; Kourkoulos, D.; Hertel, D.; Meerholz, K.; De Cola, L. *Angew. Chem., Int. Ed.* **2011**, *50*, 946−950. (h) Klawonn, T.; Gansäuer, A.; Winkler, I.; Lauterbach, T.; Franke, D.; Nolte, R. J. M.; Feiters, M. C.; Börner, H.; Hentschel, J.; Dötz, K. H. *Chem. Commun.* **2007**, 1894−1895.

(15) (a) Bull, S. R.; Guler, M. O.; Bras, R. E.; Meade, T. J.; Stupp, S. I. *Nano Lett.* **2005**, *5*, 1−4. (b) Kim, H.-J.; Lee, J.-H.; Lee, M. *Angew. Chem., Int. Ed.* **2005**, *44*, 5810−5814. (c) Naota, T.; Koori, H. *J. Am. Chem. Soc.* **2005**, *127*, 9324−9325. (d) Ziessel, R.; Pickaert, G.; Camerel, F.; Donnio, B.; Guilon, D.; Cesario, M.; Prangé, T. *J. Am. Chem. Soc.* **2004**, *126*, 12403−12413. (e) Sohna, J.-E.; Fages, F. *Chem. Commun.* **1997**, 327−328. (f) Kawano, S.-i.; Fujita, N.; Shinkai, S. *J. Am. Chem. Soc.* **2004**, *126*, 8592−8593. (g) Beck, J. B.; Rowan, S. J. *J. Am. Chem. Soc.* **2003**, *125*, 13922−13923. (h) Shirakawa, M.; Fujita, N.; Tani, T.; Kaneko, K.; Shinkai, S. *Chem. Commun.* **2005**, 4149−4151. (i) Kishimura, A.; Yamashita, T.; Aida, T. *J. Am. Chem. Soc.* **2005**, *127*, 179−183. (j) Kishimura, A.; Yamashita, T.; Yamaguchi, K.; Aida, T. *Nat. Mater.* **2005**, *4*, 546−549. (k) Roubeau, O.; Colin, A.; Schmitt, V.; Clérac, R. *Angew. Chem., Int. Ed.* **2004**, *43*, 3283−3286. (l) Kuroiwa, K.; Shibata, T.; Takada, A.; Nemoto, N.; Kimizuka, N. *J. Am. Chem. Soc.* **2004**, *126*, 2016−2021. (m) Xing, B.; Choi, M.-F.; Xu, B. *Chem.—Eur. J.* **2002**, *8*, 5028−5032. (n) Miravet, J. F.; Escuder, B. *Chem. Commun.* **2005**, 5796−5798. (o) Bühler, G.; Feiters, M. C.; Nolte, R. J. M.; DItz, K. H. *Angew. Chem., Int. Ed.* **2003**, *42*, 2494−2497. (p) de Hatten, X.; Bell, N.; Yufa, N.; Christmann, G.; Nitschke, J. R. *J. Am. Chem. Soc.* **2011**, *133*, 3158−3164.